KAPL-4761
UC-904, Materials

FATIGUE CRACK GROWTH RATE STUDIES OF MEDIUM SULFUR LOW ALLOY STEELS TESTED IN HIGH TEMPERATURE WATER

TA Auten, SZ Hayden

The Knolls Atomic Power Laboratory
Schenectady, New York 12301-1072

and
RH Emanuelson

The Babcock & Wilcox Company
Alliance, Ohio 44601

May 1993

Prepared by

KNOLLS ATOMIC POWER LABORATORY
Schenectady, New York

DISCLAIMER

CONTENTS

Page

ABSTRACT 1

INTRODUCTION 1

EXPERIMENTAL PROCEDURES 1

RESULTS 2

DISCUSSION 4

CONCLUSIONS 6

ACKNOWLEDGEMENTS 6

REFERENCES 6

Figure Number	Title	Page
1	FCGR as a Function of Applied Δ K at 260C	2
2	FCGR as a Function of Applied Δ K at 149C	2
3	FCGR Test of No. CA5-09 in Oxygenated Water	4
4	Time-Based FCGR Data for 260C	4
5	Time-Based FCGR Data for 149C	5
6	Summary of the Corrosion Potential Data for the Present Tests	5
7	Area Fraction (%) of MNS Inclusions vs Sulfur Content	5

CONTENTS (Cont'd)

Table Number	Title	Page
I	Ladle Analysis for the Twc Forgings	1
II	Test Water Analysis	2
III	FCGR Data Results for the Individual Tests	3

FATIGUE CRACK GROWTH RATE STUDIES OF MEDIUM SULFUR LOW ALLOY STEELS TESTED IN HIGH TEMPERATURE WATER

TA Auten, SZ Hayden

The Knolls Atomic Power Laboratory
Schenectady, New York 12301-1072

and
RH Emanuelson

The Babcock & Wilcox Company
Alliance, Ohio 44601

Abstract

Fatigue crack propagation tests of medium sulfur (0.007 to 0.011 wt%) ASTM A508-Class 2 forgings were performed in deaerated high purity, high temperature water. In general, these forgings did not exhibit environmentally assisted cracking (EAC) in tests at 149°C (300°F) or at 260°C (500°F). Lowering the pH did not raise the crack growth rates significantly. However, adding a small amount of oxygenated water to the feedwater increased the fatigue crack growth rates (FCGR) by a factor of about 4. Automated analyses of the sulfide inclusions in polished sections of the forgings supported a previously proposed relationship for susceptibility to EAC.

Introduction

A series of FCGR tests in high purity, high temperature water were performed on two forgings of ASTM A508 Class 2 steel. The objective of these tests was to determine if the forgings would exhibit EAC. Conventional true corrosion fatigue crack growth produces FCGR only about three times the rates expected in air. EAC rates are usually 10 to 20 times the crack growth rates in air (1-4). Most of these tests were conducted in a single water condition under a variety of load ranges with sawtooth load cycling waveforms. The forgings were tested in several locations to test for possible effects of sulfur macrosegregation. After the baseline behavior was established, one of the forgings was tested with reduced pH and also with increased dissolved oxygen content in the water.

Experimental Procedures

The test materials were taken from Forging No. 125H506VA1 ("Forging A") and from Forging No. 124H510VA1 ("Forging B"), which had the ladle analyses shown in the table below. Local check analyses gave sulfur between 0.007 and 0.011%, which is in the medium sulfur range (0.005 to 0.0125%) (1).

Compact tension specimens were machined to standard 2T dimensions with the thickness, B, of 51 mm (5). Most of the specimens were oriented for crack growth parallel to the major tensile strain during forging, which is the "T-L" orientation in the fracture toughness test standard (6). The exceptions were No. CA5-20 with an L-T orientation and No. CA5-21 with an L-S, both of which came from Forging B.

In an effort to detect possible effects of macrosegregation (or "ingot pattern" segregation) of sulfur, specimens were machined from several different locations within Forging A. First, specimens were taken from cores (material removed to facilitate subsequent fabrication) from two different positions about 10 ft apart along the length of the forging. These cores correspond roughly to the mid-height position of the original cast ingot and are labelled Cores 6 and 9 in Table II. Second, specimens were taken from the upper prolongation of the forging, which corresponds to the top-height position of the original ingot, exclusive of any shrinkage zone material removed prior to forging. Roughly speaking, higher ingot positions are more likely to have higher sulfur contents due to segregation. Finally, the specimens were tracked for position with respect to thickness through the forging wall. One of the forging surfaces, called the "inner" surface, came from material that was close to the centerline of the original ingot, while the "outer" surface of the forging came from the outside region of the original ingot. Segregation increases the concentration of sulfur from the outside toward the ingot centerline.

Specimens were also machined from several different locations within Forging B as part of the effort to detect effects of macrosegregation. Only one core (corresponding to the mid-height of the original ingot) was available from this forging. Also, specimens were taken from the upper and lower prolongations of the forging. While the upper prolongation again corresponds to the top-height position of the ingot, the lower prolongation corresponds to the bottom, where the sulfur contents should be relatively low due to negative segregation.

Almost all of the tests were performed at the Alliance Research Center of the Babcock & Wilcox Company in Alliance, Ohio. The autoclave was made of AISI Type 316 stainless steel and had a 0.076 m^3 (20 gallon) capacity. The water supply was operated as a once-through refreshed system with a flow rate of 2.1 to 2.6 E-7 m^3sec^{-1} (0.20 to 0.25 gal/hour). High purity deaerated water was prepared to the desired chemistry and stored in a stainless steel reservoir with a cover gas of high purity (99.99%) hydrogen. The nominal effluent water composition is given in Table II.

Once the specimen, displacement gage, corrosion potential coupon, and other parts of the test system had been assembled, the autoclave vessel was brought into position and sealed. The vessel was then purged with pure nitrogen gas and held for several hours.

Table I. Ladle Analyses for the Two Forgings

FORGING	C	Mn	P	S	Si	Ni	Cr	V	Mo
A	0.22	0.60	0.008	0.013	0.26	0.70	0.38	0.01	0.62
B	0.21	0.65	0.008	0.012	0.27	0.71	0.36	<0.01	0.62

Table II. Test Water Analysis

Oxygen	8 ppb
Hydrogen	28 std cc/kg H_2O
Chloride	13 ppb
Fluoride	10 ppb
Total Organic Carbon	340 ppb
Trace Metals	< 100 ppb each
pH (at room temperature)	10.2
Conductivity	45 μS/cm.

At that point, the vessel was filled with the prepared deaerated water from the feedwater tank, pressurized and heated. Testing began approximately 24 hours after the system reached the target temperature.

Some tests were performed on Specimen CA5-09 with oxygenated water injected into the inlet side of the autoclave. The main feedwater tank used a pure nitrogen cover gas for these tests, rather than the hydrogen indicated in Table II. This system was decoupled from the autoclave for all other tests.

The corrosion potential was measured for each test for a 25 x 25 x 3 mm section machined from Forging A. This coupon was located about ½ inch from the notch tip of the specimen and was monitored by an external AgCl/KCl reference electrode.

Loads were applied to the specimens through a computer-controlled servohydraulic system. The load cell was mounted outside the autoclave, and a displacement transducer was attached directly to the specimen. Specimen compliance was used to estimate the crack lengths and to control the tests to maintain constant values of ΔK throughout the test. Several constant ΔK tests were run on each specimen. Each test was continued for about 0.5 mm crack extension. The loadings for each of the tests are listed in Table III. A few of the tests (Specimens CA5-31, CA5-32, CA5-33, and TR-1 in Table III) were performed at the Knolls Atomic Power Laboratory (KAPL). These specimens had 2T planar dimensions, but were only 25 mm thick. The water chemistry was the same as in Table II. However, the water flow was high enough to exchange the same water volume in about one day, rather than three.

Results

Table III lists the FCGR data for each of the tests. These results are displayed in Figures 1 and 2 as FCGR *vs.* the range of applied ΔK for the tests at 260°C and 149°C, respectively. In Figure 1 the results at 260°C are shown for both forgings at load ratios, R, (= minimum load/maximum load) of 0.3 and 0.7. Also shown in this figure are the best-fit curves for crack extension in mm/cycle for a large database for low alloy steels in air (2):

$$\frac{da}{dN} = 7.87 \cdot 10^{-8} \left(\frac{\Delta K}{2.88\text{-}R} \right)^{3.07} \qquad (1)$$

where ΔK is the applied stress intensity factor range in MPa√m. None of the data points in Figure 1 fall below the corresponding best-fit lines, indicating that the water environment did have some effect. However, in no case did the FCGR fall more than a factor of 3 above the lines.

The tests at 149°C were to check temperature sensitivity; the results are plotted in Figure 2. One of these points fell below the Equation 1 line, while all the other points were clearly above it. Also, one result was a factor of about 7 times greater than the Equation 1 value. The low data point appears to be the result of loading sequence effects in the series of tests on Specimen CA5-01; Table III lists the tests in the order performed, *i.e.*, the order of the ΔK tests for CA5-01 was 58.3, 23.1, 33.0, and 42.9 Mpa√m. This sequence avoided applying the highest ΔK when

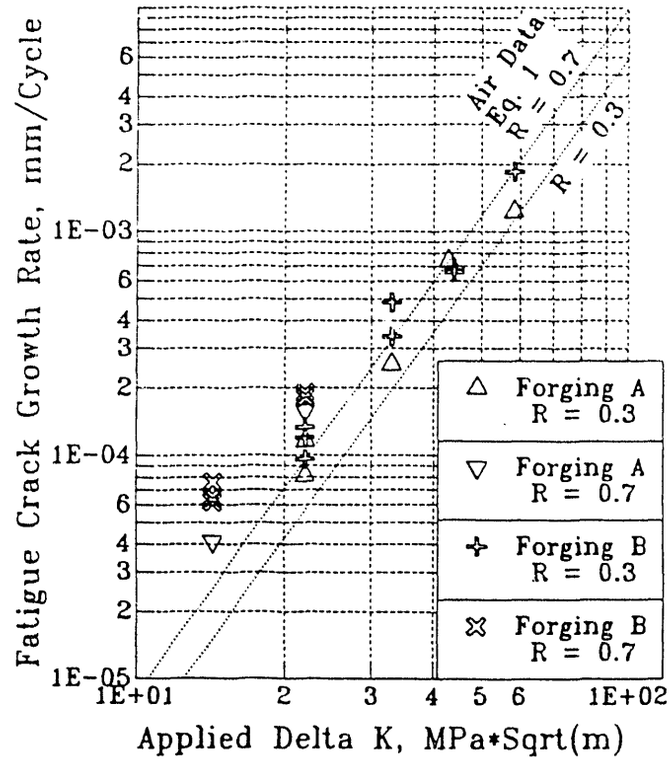

Figure 1. FCGR as a Function of Applied ΔK at 260°C.

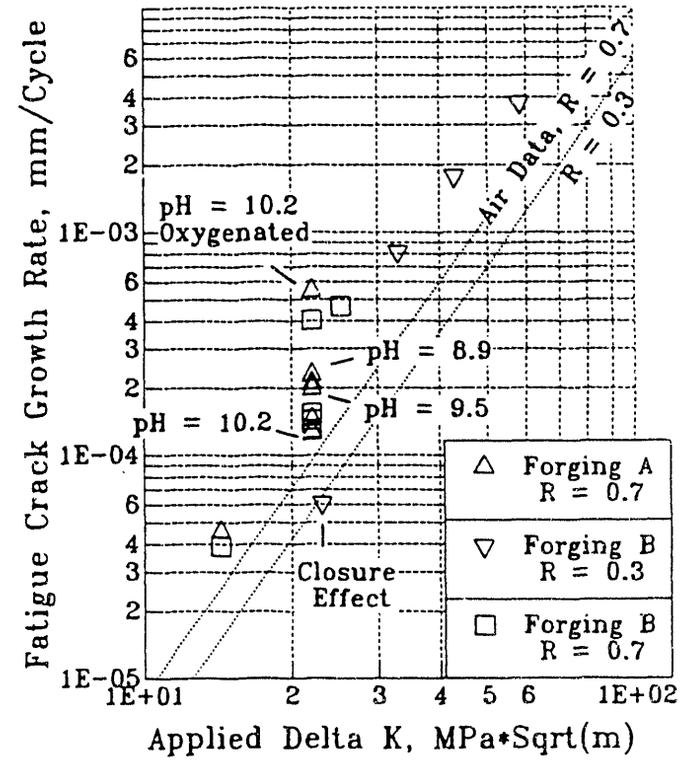

Figure 2. FCGR as a Function of Applied ΔK at 149°C.

Table III. FCGR Data Results for the Individual Tests

Specimen Number / Forging / Location in Forging	ΔK Range Mpa√m	Load Ratio	Rise Time sec	FCGR mm/cycle	Crack Tip Speeds Measured mm/sec	Baseline mm/sec
A. Tests at 260°C (Nos. CA5-31, TR-1, CA5-32, and CA5-33 at 243°C):						
CA5-02 / Forging B	44.0	0.3	51	6.58 E-4	1.29 E-5	9.30 E-6
Upper Prolongation	33.0	0.3	51	3.40 E-4	6.67 E-6	3.84 E-6
CA5-04 / Forging B	22.0	0.3	51	1.33 E-4	2.61 E-6	1.10 E-6
Core	58.3	0.3	51	1.85 E-3	3.63 E-5	2.21 E-5
	33.0	0.3	51	4.42 E-4	8.66 E-6	3.84 E-6
CA5-06 / Forging B	14.3	0.7	102	7.59 E-5	7.44 E-7	2.47 E-7
Lower Prolongation	22.0	0.7	51	1.81 E-4	3.56 E-6	1.86 E-6
CA5-08 / Forging A	22.0	0.3	51	1.16 E-4	2.21 E-6	1.10 E-6
Upper Prolongation	58.3	0.3	51	1.23 E-3	2.41 E-5	2.21 E-5
	33.0	0.3	51	2.56 E-4	5.03 E-6	3.84 E-6
	42.9	0.3	51	7.43 E-4	1.46 E-5	8.60 E-6
CA5-19 / Forging A	14.3	0.7	102	4.11 E-5	4.03 E-7	2.47 E-7
Core 9	22.0	0.7	102	1.58 E-4	1.55 E-6	9.29 E-7
CA5-20 / Forging B	14.3	0.7	102	6.20 E-5	6.08 E-7	2.47 E-7
Core, LT Orientation	22.0	0.7	102	1.82 E-4	1.78 E-6	9.29 E-7
CA5-21 / Forging B	14.3	0.7	102	6.48 E-5	6.35 E-7	2.47 E-7
Core, LS Orientation	22.0	0.7	102	1.91 E-4	1.88 E-6	9.29 E-7
CA5-31 / Forging A Core 6	22.0	0.3	51	8.1 E-5	1.6 E-6	1.1 E-6
TR-1 / Forging B Upper Prolongation	22.0	0.3	51	9.6 E-5	1.9 E-6	1.1 E-6
CA5-32 / Forging B Upper Prolongation	22.0	0.3	51	1.2 E-4	2.4 E-6	1.1 E-6
CA5-33 / Forging B Upper Prolongation	44.0	0.3	51	6.9 E-4	1.3 E-5	9.3 E-6
B. Tests at 149°C:						
CA5-01 / Forging B	58.3	0.3	30	3.78 E-3	1.26 E-4	3.75 E-5
Upper Prolongation	23.1	0.3	30	6.10 E-5	2.03 E-6	2.19 E-6
	33.0	0.3	30	8.18 E-4	2.73 E-5	6.54 E-6
	42.9	0.3	30	1.78 E-3	5.93 E-5	1.46 E-5
CA5-03 / Forging B	25.3	0.7	51	4.65 E-4	9.11 E-6	2.85 E-6
Core	22.0	0.7	51	4.04 E-4	7.92 E-6	1.86 E-6
	22.0	0.7	300	1.54 E-4	5.15 E-7	3.16 E-7
	22.0	0.7	100	1.30 E-4	1.30 E-6	9.47 E-7
CA5-05 / Forging B	14.3	0.7	102	3.91 E-5	3.83 E-7	2.47 E-7
Lower Prolongation	22.0	0.7	51	1.44 E-4	2.81 E-6	1.86 E-6
CA5-07 / Forging A	14.3	0.7	102	4.55 E-5	4.45 E-7	2.47 E-7
Upper Prolongation	22.0	0.7	51	2.10 E-4	4.30 E-6	1.86 E-6
	22.0	0.7	102	1.45 E-4	1.43 E-6	9.29 E-7
CA5-09 / Forging A / Core 6						
pH = 10.2:	22.0	0.7	102	1.28 E-4	1.25 E-6	9.29 E-7
pH = 9.5:	22.0	0.7	102	2.00 E-4	1.96 E-6	9.29 E-7
pH = 8.9:	22.0	0.7	102	2.30 E-4	2.25 E-6	9.29 E-7
pH = 10.2: (with oxygenated water)	22.0	0.7	102	5.46 E-4	5.35 E-6	9.29 E-7

the remaining ligament of the specimen was at its smallest. The load shedding to get from a ΔK of 58.3 down to 23.1 was performed with a normalized K gradient of:

$$C = (1/K)\bullet(dK/da) = -0.2\ mm^{-1} \quad (2)$$

which violates the recommended lower limit of -0.8 mm^{-1} (5). Care was taken in all subsequent tests to stay above the limit for all load-shedding steps.

The data point at the greatest distance above the baseline in Figure 2 resulted from the test of Specimen CA5-09 with oxygenated water. Several different tests were performed on this specimen, as outlined in Table III. The first test established its baseline FCGR for ΔK = 22 Mpa$\sqrt{m}$ with the standard water conditions. Then the pH was lowered; first to pH = 9.5 and then to 8.9. The FCGR were progressively higher, Table III; but the increments were too small to be considered significant.

For the final test on Specimen CA5-09, the pH was brought back to 10.2, and trials of the system for oxygen addition were performed. As a first attempt, oxygen was introduced with all other conditions maintained, *i.e.*, hydrogen was used as the cover gas in the feedwater tank. The system was operated for about 12 days before oxygenated water was pumped into the autoclave. The oxygen content of the water rose to more than 300 ppb about 2 days later. Adjustments in the oxygen level were attempted by changing the inlet pump setting, and the oxygen level started to fall. Eventually, the oxygen analyses fell below 10 ppb, in spite of repeated increases in the inlet flow rate of oxygenated water. Apparently, the hydrogen cover gas pressure was sufficient to scavenge all of the oxygen being introduced. The fact that this did not occur for several days after the introduction of the oxygen can be attributed to catalysis effects.

At this point, the cover gas for the main feedwater tank was switched to nitrogen, and all other conditions were kept the same. At first, the same behavior of the effluent oxygen content seemed to occur. However, small changes of the inflow rate of oxygenated water produced substantial changes in effluent oxygen. The effluent oxygen tracked closely with the corrosion potential. When the initial surge of effluent oxygen subsided, a steady level of about 15 ppb appeared to have been established for about two days.

Then, load cycling for the FCGR test began; Figure 3 shows the variation of the effluent oxygen content, the effluent flow rate, the autoclave corrosion potential, and the specimen crack length as a function of load cycles during the test. The oxygen content of the effluent water varied from approximately 15 to 290 ppb with the corrosion potential tracking closely. Yet, the fatigue crack grew at a remarkably steady rate.

Discussion

Time-based plots are used here as a convenient way to assess the effects of variations in the frequency and waveform of the load cycles in water environments (1). The crack tip speed measured during the test in the water environment, $\dot{a}_c$, is calculated by dividing the measured crack growth rate in mm/cycle by the rise time per cycle in seconds:

$$\dot{a}_c = \frac{da}{dN \bullet t_R} \quad (3)$$

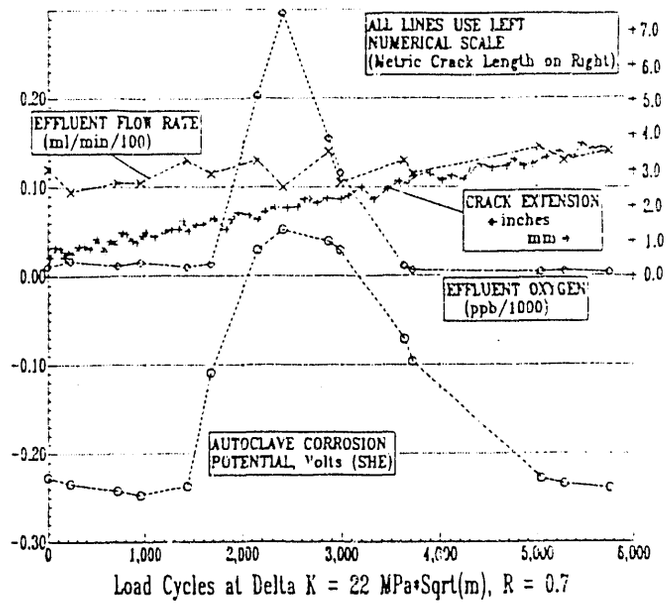

Figure 3. FCGR Test of No. CA5-09 in Oxygenated Water.

These crack tip speeds are compared with baseline speeds, $\dot{a}_b$, for tests in air (2). The baseline crack tip speeds are calculated from a best-fit curve through a large database of fatigue crack growth rates for low alloy steels in air at 288°C divided by the rise time:

$$\dot{a}_b = \frac{7.87 \bullet 10^{-5}}{t_R}\left(\frac{\Delta K}{2.88\text{-}R}\right)^{3.07} \quad (4)$$

where $\dot{a}_b$ is in mm/sec and ΔK is in Mpa$\sqrt{m}$.

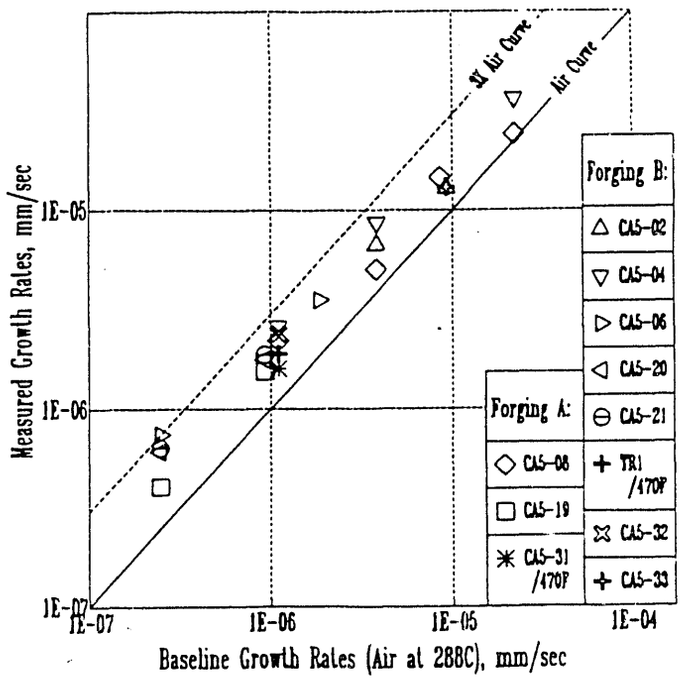

Figure 4. Time-based FCGR Data for 260°C.

If there is no effect of the environment, then a plot of the $\dot{a}_e$ data against $\dot{a}_b$ should result in a clustering of the points about the line $\dot{a}_e = \dot{a}_b$. Note that the time-based plot also normalizes the data for the effect of load ratio, R,.that is, all the data should fit the same line, regardless of the load ratio. In fact, even low alloy steels with sulfur contents < 0.005% tend to produce crack tip speeds that lie somewhat above this line (1).

Figure 4 is a time-based plot of the fatigue crack growth rates from the present tests at 243 and 260°C. None of the data fell below the air baseline; rather, all the points except one lie between the baseline and the parallel line $\dot{a}_e = 3 \bullet \dot{a}_b$, which is identified in Figure 4. This line is shown to provide a gage for comparison of the present results with earlier studies. It is clear that these data do not show the large increases in FCGR observed by Van Der Sluys, et al. (9). Their data for 0.021% sulfur steel exhibited $\dot{a}_e$ levels that were greater than $\dot{a}_b$ by an order of magnitude or more.

Note also that the four tests performed at KAPL (Specimens TR-1, CA5-32, CA5-33, and CA5-31) produced growth rates that fall among the results obtained at the B&W facility.

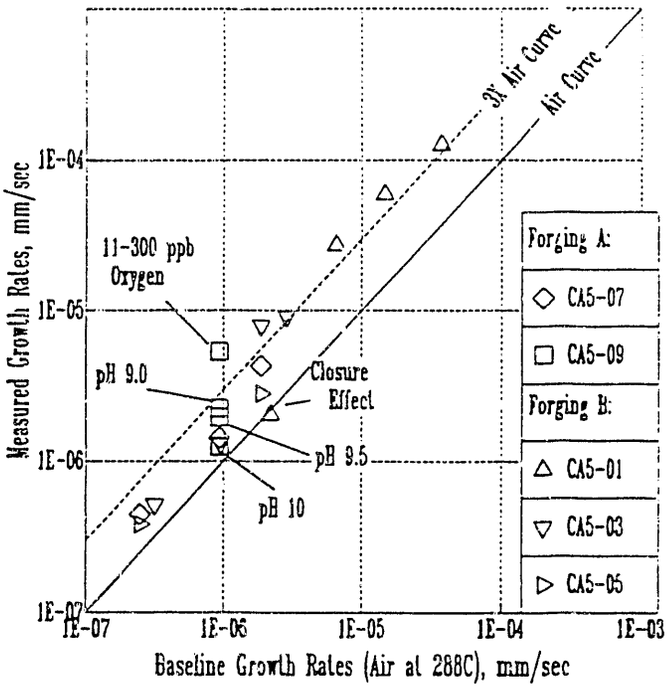

Figure 5. Time-based FCGR Data for 149°C.

The plot of time-based rates in Figure 5 shows that the tests at 149°C tended to yield higher growth rates than at 260°C. Six of the 149°C tests yielded growth rates above the $\dot{a}_e = 3 \bullet \dot{a}_b$ line. As shown in Figure 6, the corrosion potential for the tests at 149°C (approximately -635 mv) averaged somewhat higher than at 260°C (approximately -690 mv). This prompted the decision to test for the effects of lowered pH and of elevated oxygen at 149°C under the assumption that the higher corrosion potential would increase the chances of encountering EAC. The high oxygen test of specimen CA5-09 did produce a growth rate above the $\dot{a}_e = 3 \bullet \dot{a}_b$ line, but the tests at lower pH did not. At pH = 10.2, $\dot{a}_e$ = 9 E-7 mm/cycle. The tests at pH = 9.5 and 8.9 at the same baseline tip speed produced FCGR higher by factors of 1.6 and 1.8, respectively, than the growth rate at pH 10.2, well below the increases normally associated with EAC (> >3X).

The addition of a small amount of oxygenated water to the feedwater in the last test of Specimen CA5-09 at 149°C produced erratic corrosion potentials, ranging from -0.247 to +0.039 volts. Throughout this period, the FCGR remained steady at $\dot{a}_e$ = 5.35

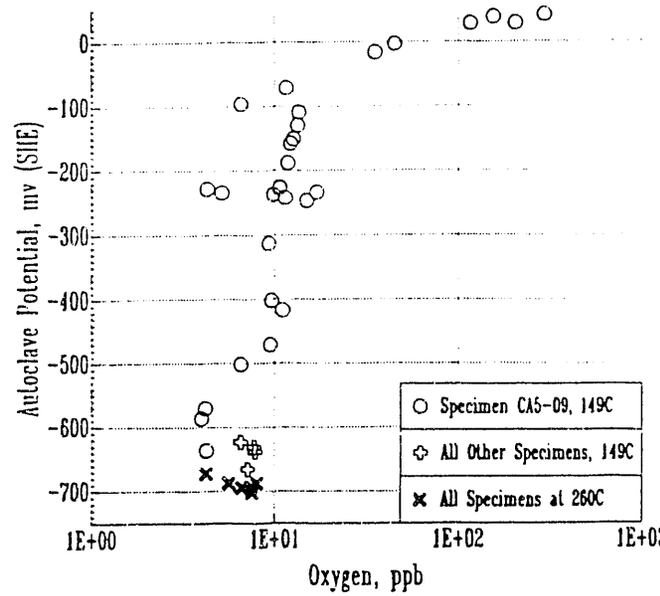

Figure 6. Summary of the Corrosion Potential Data for the Present Tests. The Solid Data Points Correspond to Tests at 260C.

E-6 mm/sec, an increase by a factor of 4.3 over the $\dot{a}_e$ at pH 10.2. This growth rate was a factor of 5.8 greater than the baseline air growth rate. This was still lower than the factor of 10 to 20 suggested as the definition of EAC in the introduction to this paper. Other workers have shown that corrosion potential has a controlling influence on the fatigue crack growth rates in high temperature water testing (4,7). Indeed, the results in Reference 4 seem to suggest that once the potential exceeds about -250 mv, EAC occurs, which would be consistent with the results for Specimen CA5-09.

The corrosion potential data recorded throughout these tests is plotted against the associated oxygen analyses in Figure 6. The average corrosion potentials for the B&W tests at 149°C ranged from -0.665 to -0.623 v, while those at 260°C produced -0.702 to -0.672 v. The shape of the curve follows that published for Type 304 stainless steel (8).

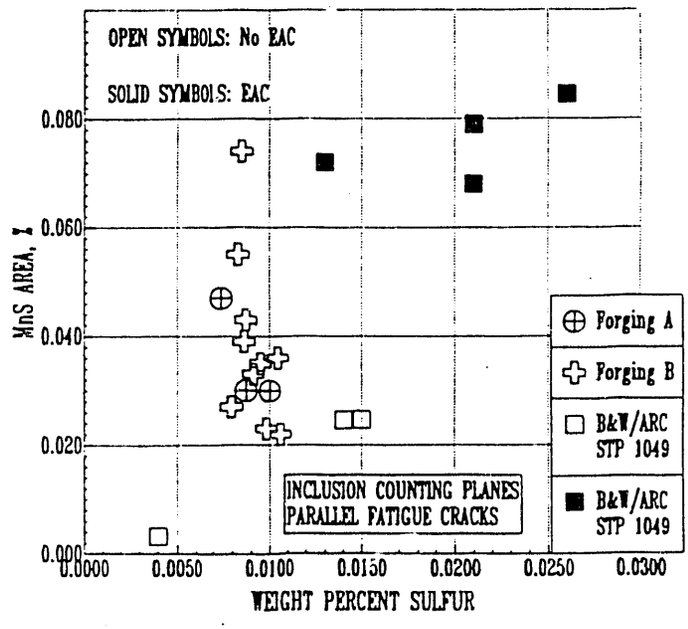

Figure 7. Area Fraction (%) of MnS Inclusions *vs.* Sulfur Content. The present data are based on local sulfur analyses, while the earlier data utilize ladle sulfur.

The fracture surfaces of all of the tested specimens had smooth thumbnail shapes. Although the fatigue cracks encountered occasional sulfides, no shape instabilities in the thumbnail crack fronts were observed. This fact, together with the lack of any fatigue crack growth rates that were close to an order of magnitude greater than the baseline air FCGR, suggests that no EAC has occurred in these tests.

The general absence of any large increases in growth rates for any of the specimens from either forging indicates that either macrosegregation has had no effect or that the extent of macrosegregation is small. Since the range of the sulfur analyses made on sections removed from the test specimens was 0.007 to 0.014 weight percent sulfur, it appears that only limited macrosegregation existed in these two forgings.

Specimens CA5-04, CA5-20, and CA5-21 provide comparisons of different crack orientations from the same core from Forging B. Again, no accelerated growth occurred; so, orientation appears to have no effect for medium sulfur steel.

Quantitative analyses of the inclusions present in metallographic sections parallel to and roughly 1 mm below the crack planes were made on most of the test specimens on an electron microprobe operated through a particle recognition computer program. At the same time, sulfur compositions were obtained on sections cut near the fatigue precracks. The data indicate that these steels were relatively clean, as shown in Figure 7 by comparison with earlier data (9). For the present data, the points in this plot represent area fractions of sulfide inclusions counted over surface areas of roughly 10 mm^2. These counts are plotted against the local sulfur analyses for each of the FCGR test specimens. In the original publication of this figure, ladle sulfur analyses were used (9). The data suggest that some rough relationship exists between the area fraction of sulfide inclusion present in a steel and its susceptibility to EAC; perhaps the conclusion would be that materials with sulfide inclusion area fractions greater than 0.00050 will exhibit EAC in high purity water. The present data suggest that the line should be drawn at an area fraction of 0.00060, although one of the results from Forging B lies just above that level. It may be reasonable to average that point with the rest of the data for this forging.

In summary, these two medium sulfur forgings did not exhibit environmentally assisted cracking over a rather broad range of frequencies and ΔK values in tests in high purity water at 149°C (300°F) and at 260°C (500°F). EAC behavior was not induced through changes in location within the forgings or in orientation of the test specimens. Also, changes in the pH from about 10.2 to 9.0 and increases in the oxygen content of the water did not induce EAC, although the latter did increase the fatigue crack growth rates by a factor of about 4. The lack of instabilities in the shapes of the fatigue crack fronts and of cleavage facets in the crack surfaces indicate that classic EAC did not occur in any of these tests, even when oxygen was added to the water. This behavior is consistent with the low inclusion content of the steel.

Conclusions

1. Two medium sulfur ASTM A508-Class 2 steel forgings did not exhibit the large increases in FCGR associated with environmentally assisted cracking (EAC) in fatigue tests at 149°C or at 260°C in high purity water.

2. Reducing the pH from 10.2 to 8.9, did not change the crack growth rates significantly.

3. The addition of oxygenated water to the feedwater drove the corrosion potential above -250 mv and increased the fatigue crack growth rates by a factor of about 4.

4. No instabilities in the shapes of the crack fronts were observed, a characteristic commonly associated with EAC behavior.

5. Area fraction measurements of inclusions near the crack planes supported a previously proposed relationship between the area fraction of sulfide inclusion present in a steel and its susceptibility to EAC.

Acknowledgements

Thanks are extended to P. L. Andresen of the General Electric Research Center, L. A. James of the Bettis Atomic Power Laboratory, C. J. Corrow of KAPL, and W. A. Van Der Sluys of the Babcock & Wilcox Research Center for their helpful discussions. We also thank several key contributors, including Ms. Sue Gwiazdowski, Gary Dansfield, Bruce Furbeck, Paul Harris, Ray Brownell, Gerry Neugebauer, V. P. Nordstrom, and D. A. Scavone. This work was performed at the Knolls Atomic Power Laboratory operated for the U. S. Department of Energy by Martin Marietta under Contract No. DE-AC12-76SN00052. Much of the work was performed by subcontract.

References

1. W. A. Van Der Sluys, E. D. Eason, and J. D. Gilman, "Environment-Sensitive Cracking of Pressure Vessel Steels", Proceedings of the Fourth International Symposium on Environmental Degradation of Materials in Nuclear Power Systems - Water Reactors, Ed. Daniel Cubicciotti, NACE, Houston, Texas (1990), 37-62.

2. E. A. Eason et al., "Analysis of Pressure Vessel Steel Fatigue Tests in Air", Nuclear Engineering and Design, 115(1)(1989), 23-30.

3. F. P. Ford and P. L. Andresen, "Corrosion Fatigue of A533B/A508 Pressure Vessel Steels in 288°C Water", Proceedings of the Third International Atomic Energy Agency Specialist's Meeting on Subcritical Crack Growth, Moscow, USSR, May 14-17, 1990, NUREG/CP-0112, (1990), 105-124.

4. J. D. Atkinson and J. E. Forrest, "The Role of MnS Inclusions in the Development of Environmentally Assisted Cracking of Nuclear Reactor Pressure Vessel Steels", Proceedings of the Second International Atomic Energy Agency Specialist's Meeting on Subcritical Crack Growth, Sendai, Japan, May 15-17, 1985, NUREG/CP-0067 (1986), 153-178.

5. "Standard Test Method for Measurement of Fatigue Crack Rates", ASTM Standard E 647-88a.

6. "Standard Test Method for Plane-Strain Fracture Toughness of Metallic Materials", ASTM Standard E 399-83.

7. H. E. Hanninen, E. Arilahti, and U. Ehrstén, "Determination of the threshold Values for Corrosion Fatigue Crack Growth Rate of Pressure Vessel Steels in PWR Primary Water", Proceedings of the Fifth International Symposium on Environmental Degradation of Materials in Nuclear Power Systems - Water Reactors, Monterey, California, NACE (1992).

8. M. E. Indig and A. R. McIlree, "High Temperature Electrochemical Studies of the Stress Corrosion Cracking of Type 304 Stainless Steel', Corrosion, 35(7)(1979), 288-295.

9. W. A. Van Der Sluys and R. H. Emanuelson, "Environmental Acceleration of Fatigue Crack Growth in Reactor Pressure Vessel Materials and Environments", Environmentally Assisted Cracking: Science and Engineering, ASTM STP 1049, eds. W.B. Lisagor et al., (1990) 117-135.

END

DATE
FILMED
11/10/93